Chapter C

Constraints on the Structure of Crater Flat, Southwest Nevada, Derived from Gravity and Magnetic Data

By Victoria E. Langenheim

Contents

Figures

Table

[For table of abbreviations and conversions, click here]

Abstract

Gravity data were modeled across Crater Flat using three distinct geometries for the Bare Mountain fault: (1) stepped, high-angle normal faults, (2) a low-angle normal fault, and (3) a single, high-angle range-front fault with interbedding of high-density alluvium in the Crater Flat basin fill. All three models fit the gravity data well and provide three distinct geometries to test the use of other geophysical methods, such as seismic reflection and refraction. Magnetic data suggest that a stepped, high-angle normal-fault geometry for Bare Mountain is more likely than the other two geometries.

Introduction

Understanding the structural framework of Crater Flat is essential for assessing seismic hazard to the potential high-level radioactive-waste repository site at Yucca Mountain, Nev. Hypotheses to explain the formation of the elliptical deep basin at Crater Flat fall into three main categories: (1) volcano-tectonic depression or caldera (Snyder and Carr, 1984), (2) detachment faulting (Hamilton, 1988), and (3) graben faulting. Geophysical data, especially gravity data, have been used to support two of these hypotheses, namely the caldera hypothesis (Snyder and Carr, 1984), and the detachment faulting mechanism (Oliver and Fox, 1993). In particular, the gravity data have been used to model the geometry of the Bare Mountain fault, a structure that places folded and faulted Precambrian and Paleozoic sedimentary rocks of Bare Mountain in juxtaposition with the alluvial deposits of Crater Flat. The Bare Mountain fault generally has been linked geometrically to faults underlying Yucca Mountain, faults that are hidden under a thick volcanic pile. This report attempts to identify limits on the possible fault geometries of the Bare Mountain fault, using gravity and magnetic data.

Geologic Setting

Crater Flat lies in the southern part of the Great Basin section of the Basin and Range physiographic province and within the Walker Lane Belt (Carr, 1974). The northern and central Great Basin is characterized by alternating north-trending ranges and valleys, whereas the topography of the Walker Lane Belt is more diverse, with lower relief and more arcuate trends. Crater Flat, located on the southwest side of the southwestern Nevada volcanic field, has been interpreted to be a caldera complex (Carr and others, 1984).

Crater Flat is an elliptical basin rimmed by Bare Mountain on the west and Yucca Mountain on the east (fig. 1). Gravity and seismic refraction data indicate that the basin fill reaches thicknesses of 3–4 km. Because the basin fill is so thick, and the two existing drill holes in Crater Flat do not penetrate entirely through it, one must look to the surrounding geology at Yucca Mountain and Bare Mountain to determine the possible geological configuration beneath Crater Flat.

The oldest rocks in the area are exposed at Bare Mountain. They consist of upper Precambrian and Paleozoic clastic and carbonate rocks. These rocks are mildly to moderately metamorphosed (Monsen and others, 1992) and complexly faulted and locally folded. One drill hole on the east side of Yucca Mountain, UE-25 p#1 (p#1 in fig. 1) penetrated Silurian dolomite at a depth of 1,244 m (Carr and others, 1986). At the northwest end of Bare Mountain, the sequence is intruded by a Cretaceous granite body that is inferred to postdate the ductile deformation observed in the Paleozoic rocks (Monsen and others, 1992). Along the east edge of Bare Mountain, north-trending quartz latite dikes dated at 13.9 Ma clearly postdate ductile deformation of the pre-Tertiary sequence (Monsen and others, 1992).

Overlying or in fault contact with pre-Tertiary rocks are voluminous Tertiary ash-fall tuffs and lava flows extruded from several volcanic centers within and adjacent to the Timber Mountain–Oasis Valley caldera complex, north of Crater Flat. Most of the volcanism occurred between 17 and 7 Ma (Byers and others, 1976). The tuff sequence exposed at Yucca Mountain is cut by numerous west-dipping, north- to northeast-trending normal faults, with consistent down-to-the-west displacements (Scott, 1990). Dips of the tuff are generally shallow, ranging from 10° to 30°. Scott (1990) has proposed the existence of a relatively shallow (1–2 km) detachment fault underlying Yucca Mountain based on these structural patterns.

In Crater Flat, the tuffs are overlain by a thin veneer of alluvium. Pliocene cinder cones and basalt flows have a general north-northeast alignment within Crater Flat. Along the southern rim of Crater Flat are exposures of Miocene basalt (dated at 10.5 Ma), which are overlain by slide breccias composed entirely of Paleozoic debris.

Gravity

Densities

Density information is critical to modeling gravity data. An abundance of density data is available for the rocks in Crater Flat and vicinity. Density logs from the two drill holes in Crater Flat and density measurements from surface samples indicate significant density contrasts among the alluvium, basalt, tuffs, and pre-Tertiary rocks. A borehole gravimeter study of USW VH-1 (VH-1 in fig. 1) at Yucca Mountain gives densities within the tuff sequence consistent with those obtained using the gamma-gamma method (Snyder and Carr, 1984), indicating that the gamma-gamma method is an appropriate technique for measuring densities in this area, even though a smaller volume of rock is sampled in the drill hole than in the borehole gravimeter technique. Snyder and Carr (1984) determined that density and depth had the following empirical relation:

$$r = 0.26d + 1.9$$

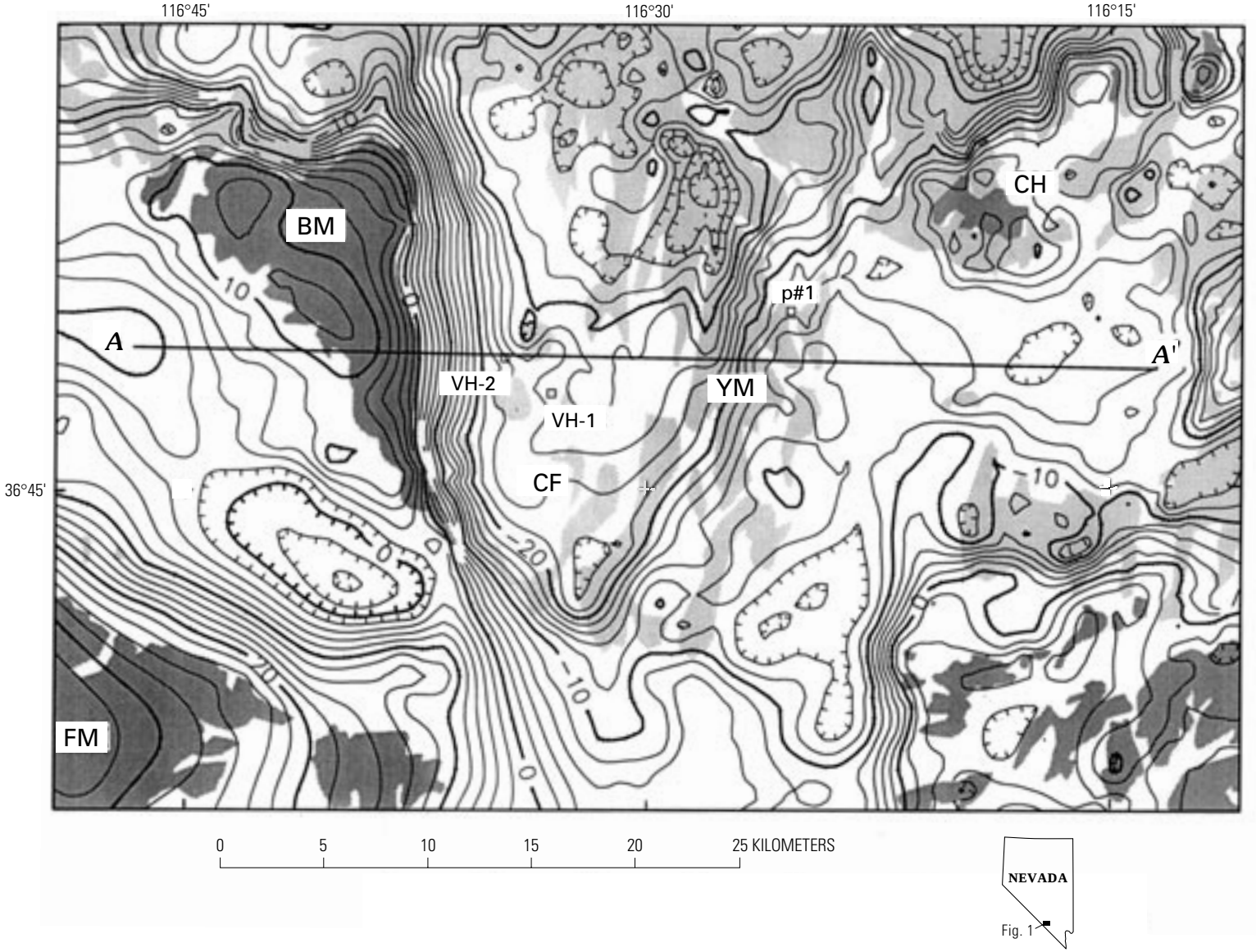

Figure 1. Isostatic gravity map of Crater Flat and vicinity. Contour interval 2 milligals. Hachures indicate gravity lows. Darker shade, Precambrian and Paleozoic rocks; light shade, Tertiary and Quaternary volcanic rocks; unshaded, Quaternary alluvium. Small square, location of drill holes USW VH-1 (VH-1), USW VH-2 (VH-2), and UE-25 p#1 (p#1). *A-A′* shows location of profiles modeled in figure 2*A-C*. BM, Bare Mountain; CF, Crater Flat; CH, Calico Hills; FM, Funeral Mountains; YM, Yucca Mountain.

where *r* is density in grams per cubic centimeter and *d* is depth in kilometers. They (Snyder and Carr, 1984) attributed the steady increase in density to closure of pore spaces and fractures and increasing alteration rather than any systematic change in lithology. This result generally holds true for the density logs of USW VH-1 and USW VH-2 except where high concentrations of Paleozoic rock fragments were present. At USW VH-2 (fig. 1), two intervals (51 and 61 m thick) of Paleozoic slide breccia have densities of 2.5–2.6 g/cm^3, which is significantly higher than densities measured for the underlying and overlying tuffs (2.0–2.3 g/cm^3) and alluvium (1.8–2.0 g/cm^3) (Carr and Parrish, 1985; Nelson and others, 1991). Similar breccias composed solely of Paleozoic debris crop out along the south edge of Crater Flat, with exposed thicknesses of at least 100 m (Swadley and Carr, 1987).

Information on the densities of the pre-Tertiary rocks is limited to density log data from UE-25 p#1, where the average density of the carbonate sequence is about 2.75 g/cm^3 (Healey and others, 1984). Densities of 77 hand samples of several different lithologies from Bare Mountain average about 2.76 g/cm^3, ranging from 2.37 g/cm^3 to 2.85 g/cm^3 (table 1).

Seismic velocities also provide indirect information on densities. Ackermann and others (1988) obtained a relationship between density and velocity, although seismic velocities are considerably more sensitive to fractures than are densities and may give unreasonably low estimated densities, especially for the pre-Tertiary rocks in the uppermost 1–2 km of the crust at Yucca Mountain (Mooney and Schapper, 1995).

Gravity Data

More than 3,000 gravity stations taken from Saltus (1988) and Harris and others (1989) were used to generate the gravity map (fig. 1). The gravity data were reduced using standard methods to complete Bouguer gravity anomalies at a reduction density of 2.67 g/cm^3 (Telford and others, 1976). This density value was chosen to emphasize the contribution to the gravity field from the topography of the Paleozoic surface and may not adequately correct for topography consisting of lower density volcanic material. The data include earth-tide, instrument drift, free-air, Bouguer, latitude, curvature, and terrain corrections. A regional correction using the principle of isostasy was also applied to the data to remove any long-wavelength effects of the mantle-crust interface compensating for topographic loads (Simpson and others, 1986).

Models

The gravity data were simulated using three distinct geometries along a profile (*A*-*A*′, fig. 1) that nearly coincides with the Yucca Mountain seismic refraction profile (Mooney and Schapper, 1995). Standard two-dimensional methods (Saltus and Blakely, 1993) were used. The seismic profile provides constraints on the density structure within the fill. The seismic model called for two different velocities within the pre-Tertiary sequence. The gravity model, on the other hand, suggests that one density for the pre-Tertiary sequence is sufficient to simulate the data, emphasizing the sensitivity of seismic velocities to fractures in the upper 2 km. Drill holes VH-2 and UE-25 p#1 provide information on the thickness of Cenozoic deposits (fig. 1). An examination of the gravity field and resulting model indicates that high-density Paleozoic rocks must be present near the surface east of the mapped trace of the Bare Mountain fault along the east side of Bare Mountain (see Hoisch, this volume) in order to account for the location of the gravity gradient. If the Bare Mountain fault extended to depth at a dip of 55° E. (dips vary from 45° to 75° along its strike; Monsen and others, 1992), the horizontal gradient of the gravity field should be maximized over the contact (Blakely and Simpson, 1986). Instead, three detailed profiles on the west flank of Crater Flat indicate that the maximum horizontal gravity gradient is 0.5–1.5 km east of the mapped Quaternary trace of the Bare Mountain fault. At least three geometries can account for the location of the maximum horizontal gravity gradient: (1) one or more steps in the steep, east-dipping fault observed at the range front of Bare Mountain (fig. 2*A*), (2) a flattening of the dip of the Bare Mountain fault (fig. 2*B*), or (3) a steeply dipping fault that incorporates high-density Paleozoic breccia within the sedimentary fill of Crater Flat at the base of the fault (fig. 2*C*).

The step model (fig. 2*A*) fits the gravity data quite well. Along the profile, the step is 1 km long and about 400 m high. Models along other profiles indicate that the step ranges in length from less than 1 km to more than 2 km. Snyder and Carr (1984) interpreted the geometry of the step model as

Table 1. Physical property measurements of Bare Mountain samples.

[g/cm^3, grams per cubic centimeter]

Lithology	Number of samples	Average density (g/cm^3)	Range in density (g/cm^3)	k[1]
Limestone	27	2.76	2.37–2.85	0–0.08
Dolomite	19	2.78	2.66–2.85	0–0.32
Breccia	3	2.71	2.62–2.83	0–0.09
Meta-carbonate rocks	16	2.75	2.63–2.85	0–0.14
Meta-pelite [2]	12	2.76	2.70–2.85	0.10–11.2
All lithologies	77	2.76	2.37–2.85	0.00–11.2

[1] 10^{-3} International System units.
[2] Wood Canyon Formation.

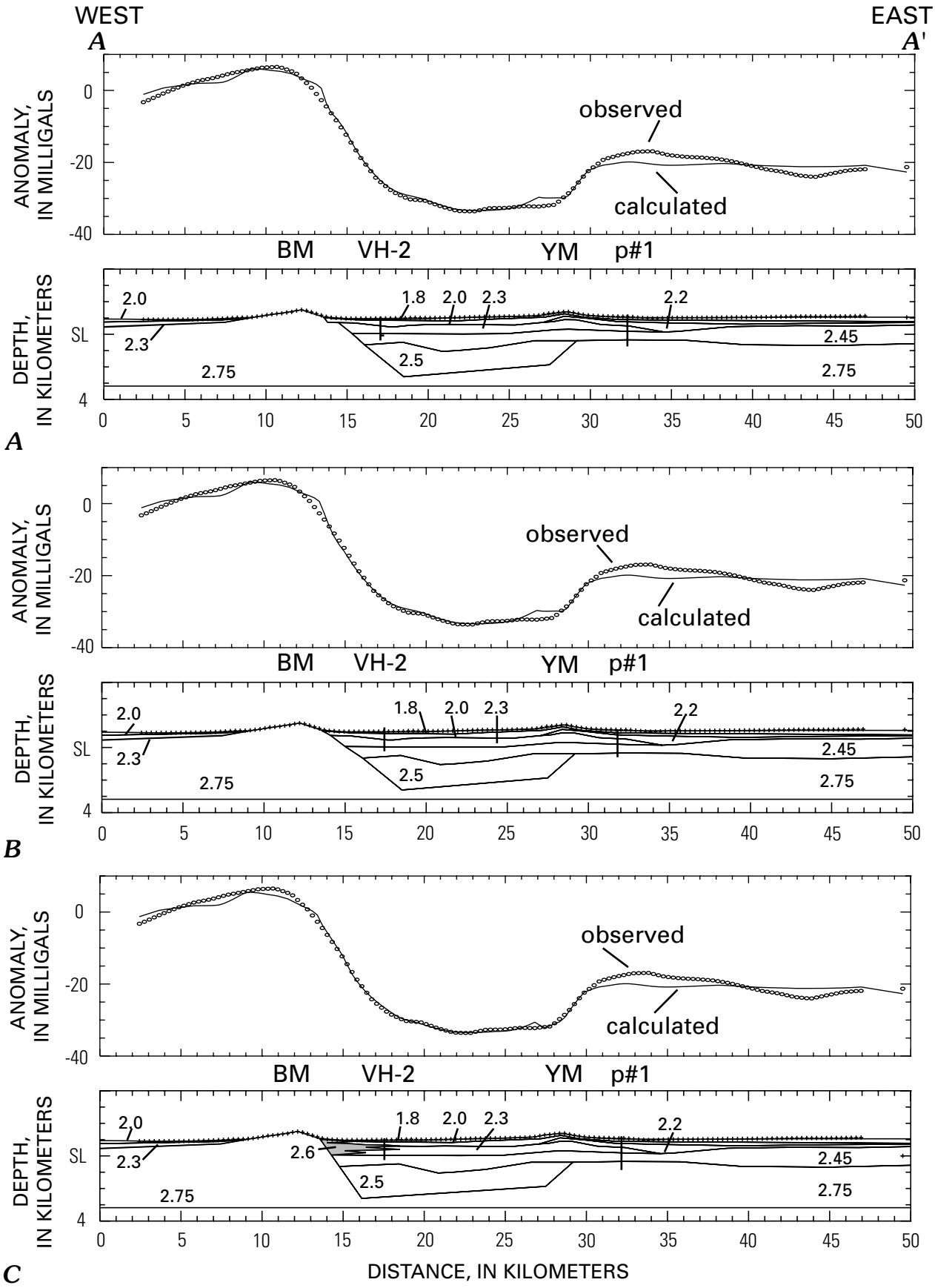

Figure 2. Two-dimensional gravity models across Crater Flat along profile *A*-*A'*. Numbers in models indicate densities in grams per cubic centimeter. Gridded values are observed gravity data. BM, Bare Mountain; YM, Yucca Mountain; VH-2, p#1, drill holes. *A*, step model, *B*, detachment fault, *C*, higher density alluvium in shaded region.

evidence for a caldera underlying Crater Flat. According to their interpretation, the Bare Mountain fault is a reactivated ring fault of the caldera that was the source of the tuffs forming the Crater Flat Group and the cause of the gravity low. This geometry may also describe a range-front fault that steps inward into the range, perhaps reflecting two major episodes of movement. This inwardly stepping normal-fault geometry has been documented in other parts of the Basin and Range province where no other evidence for a caldera structure exists (for example, Dixie Valley in Nevada, documented by Okaya and Thompson, 1985; Amargosa Desert in Nevada, documented by Brocher and others, 1993).

The gravity data can also be closely approximated by lowering the dip of the fault surface from 55° to 35° along profile *A*-*A′* (fig. 2*B*). To the north, the fault must dip even less (20°) to fit the gravity data. Oliver and Fox (1993) simulated the gravity assuming a detachment fault geometry that also includes a step in the detachment surface 3 km east of the mapped range fault. The location of their profile coincides with that of Snyder and Carr (1984). The difference between the Snyder and Carr (1984) and Oliver and Fox (1993) models is in part the result of the density distribution chosen for the basin fill. Oliver and Fox (1993) assumed a two-layer density-depth model for all of Crater Flat, whereas Snyder and Carr (1984) and the models presented here use the empirical relation between depth and density in drill hole USW VH-1. Alternatively, the smooth surface of the single, low-angle normal fault may be broken by numerous normal faults with small displacements, all down to the east.

The third geometry suggested for the Bare Mountain fault extends the steep dip measured at the surface along the Bare Mountain range fault to depth, but incorporates higher density alluvium within the basin fill (fig. 2*C*). The higher density material needs to be concentrated within the upper 1–2 km of section to fit the observed gravity gradient. Monolithologic breccias composed of Paleozoic debris crop out along the southern margin of Crater Flat. Two intervals of breccia are present in drill hole USW VH-2, more than 4 km east of the mountain front. The breccias both underlie and overlie a 10.5- to 11-Ma basalt flow. Presumably these deposits thicken towards Bare Mountain, the nearest exposure of pre-Cenozoic rocks. Carr (1984) considered these breccias to be slide breccias whose extent and age are the result of major movement on the Bare Mountain high-angle normal fault that occurred at the same time as faulting at Yucca Mountain. Alternatively, Labotka and Albee (1990) have shown that monolithologic breccias can be the result of tectonic erosion along low-angle normal faults.

The three gravity models (fig. 2) provide alternative explanations for the observed gravity gradient across the west edge of Crater Flat. The models provide target depths and geometries that can be tested with seismic reflection and refraction methods and drilling. For example, use of the seismic reflection method may determine whether extensive landslide breccias are interbedded in the upper 1–2 km of the Crater Flat fill. Analysis of detailed seismic refraction profiles parallel to the range-front fault may provide an image of the proposed step in the range-front fault because of the large velocity contrast between the low-velocity Crater Flat fill material and the higher velocity pre-Cenozoic rocks.

Magnetic Field

Magnetic Data

Total-field magnetic data from three separate surveys (U.S. Geological Survey, 1979; Langenheim and others, 1991; Grauch and others, 1993) were used to construct the aeromagnetic map shown in figure 3. The data were smoothed by upward continuation (Cordell, 1985) to an effective height of 305 m above the land surface. Data shown in figure 4 were collected with a proton-precession magnetometer with the sensor 2.4 m above the ground.

Discussion

In general, the Precambrian and Paleozoic rocks are only weakly magnetic, producing a uniform magnetic field marked by broad, low-amplitude anomalies. One exception is an intense magnetic high present over the Calico Hills (fig. 3). The source of the high appears to be altered argillite of the Devonian and Mississippian Eleana Formation, which has an average magnetization of almost 4 A/m (0.004 emu; Baldwin and Jahren, 1982). Bath and Jahren (1984) proposed that an underlying intrusion caused the alteration. The magnetic high present over the Calico Hills extends west over the northern part of Yucca Mountain, suggesting that highly magnetic argillite of the Eleana Formation (and its associated intrusion) is present at depth below Yucca Mountain and northern Crater Flat (Bath and Jahren, 1984).

The magnetic field over Bare Mountain is characterized by east-west-trending anomalies with amplitudes of more than 50 nanoteslas (nT) (fig. 3). These anomalies appear to correlate with outcrops of the Wood Canyon Formation, a Lower Cambrian unit containing siltstone, quartzite, limestone, and dolomite. Magnetic susceptibility (k) measurements confirm that the Wood Canyon Formation is indeed moderately magnetic (k=0 to 11.2, or 0 to 0.01 SI unit; table 1) whereas other formations of Paleozoic age in this region are essentially nonmagnetic. The Bare Mountain anomalies, which most likely reflect the east-west-trending structures mapped at Bare Mountain (Monsen and others, 1992), are in sharp contrast to the mostly north-south trending anomalies present to the east and north (fig. 3).

The source of most of the magnetic anomalies in figure 3 is volcanic rocks. Magnetic-property measurements of volcanic rocks in this area indicate that the remanent magnetization is the principal cause of the anomalies (Bath, 1967). The two main types of volcanic rocks that produce anomalies in the Yucca Mountain area are (1) Tertiary and Quaternary lava flows and (2) Tertiary ash-flow tuffs. Buried igneous intrusions are a third possible source. Tertiary and Quaternary lava flows tend to produce intense, irregularly shaped, isolated anomalies (Kane and Bracken, 1983). The tuffs, originally laid down as widespread ash-flow sheets, produce anomalies primarily where abrupt changes in their thicknesses or magnetization occur. This means that vertical offsets of the tuff units produce linear

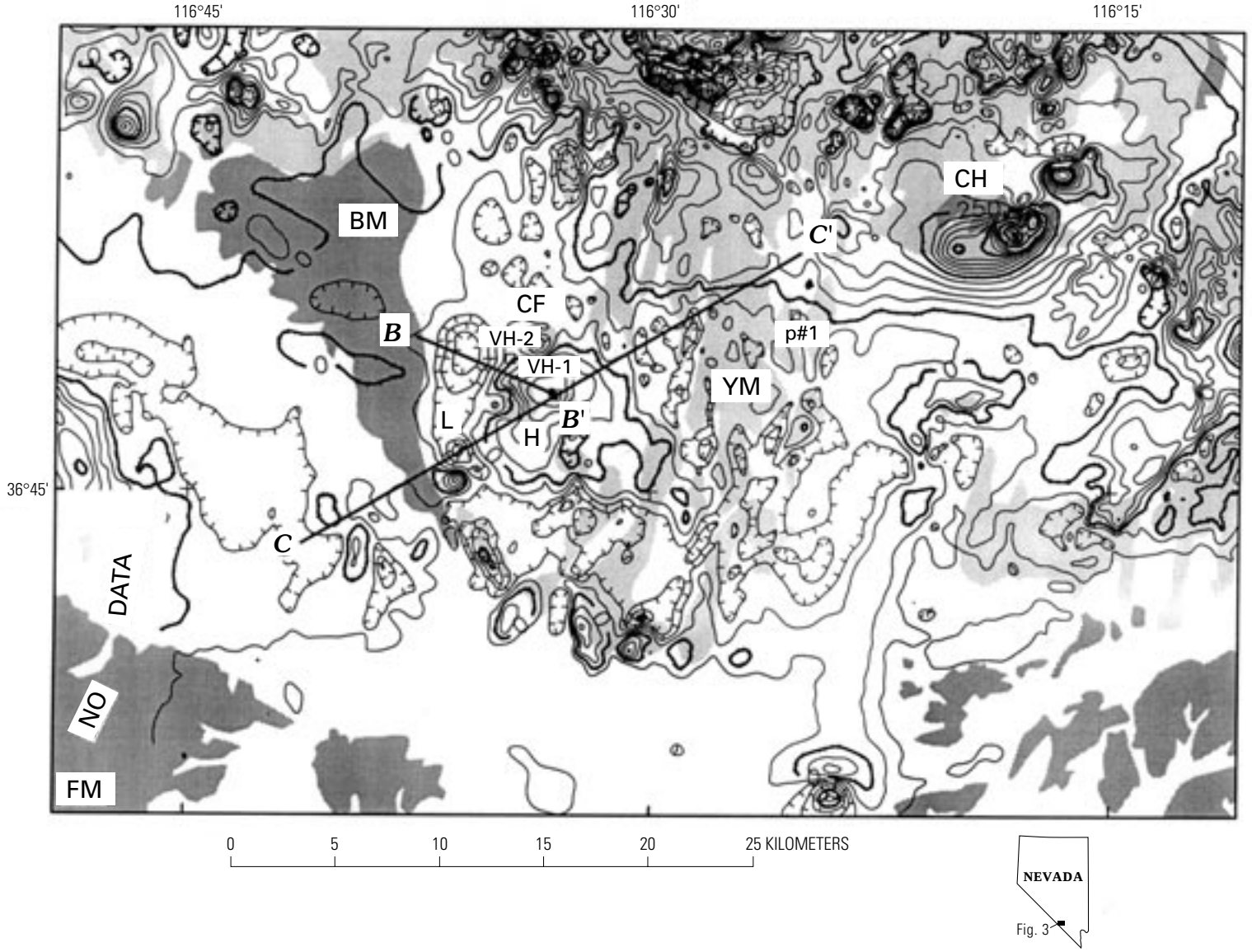

Figure 3. Aeromagnetic map of Crater Flat and vicinity. Dark shade, Precambrian and Paleozoic rocks; light shade, Tertiary and Quaternary volcanic rocks; unshaded, Quaternary alluvium. Contour interval 50 nanoteslas. Hachures indicate magnetic lows. Data from U.S. Geological Survey (1979), Langenheim and others (1991), and Grauch and others (1993). Region marked NO DATA has no high-resolution aeromagnetic coverage. L, magnetic low discussed in text; H, magnetic high. *B-B′* and *C-C′* show location of profiles in figures 4 and 5, respectively. BM, Bare Mountain; CF, Crater Flat; CH, Calico Hills; FM, Funeral Mountains; YM, Yucca Mountain.

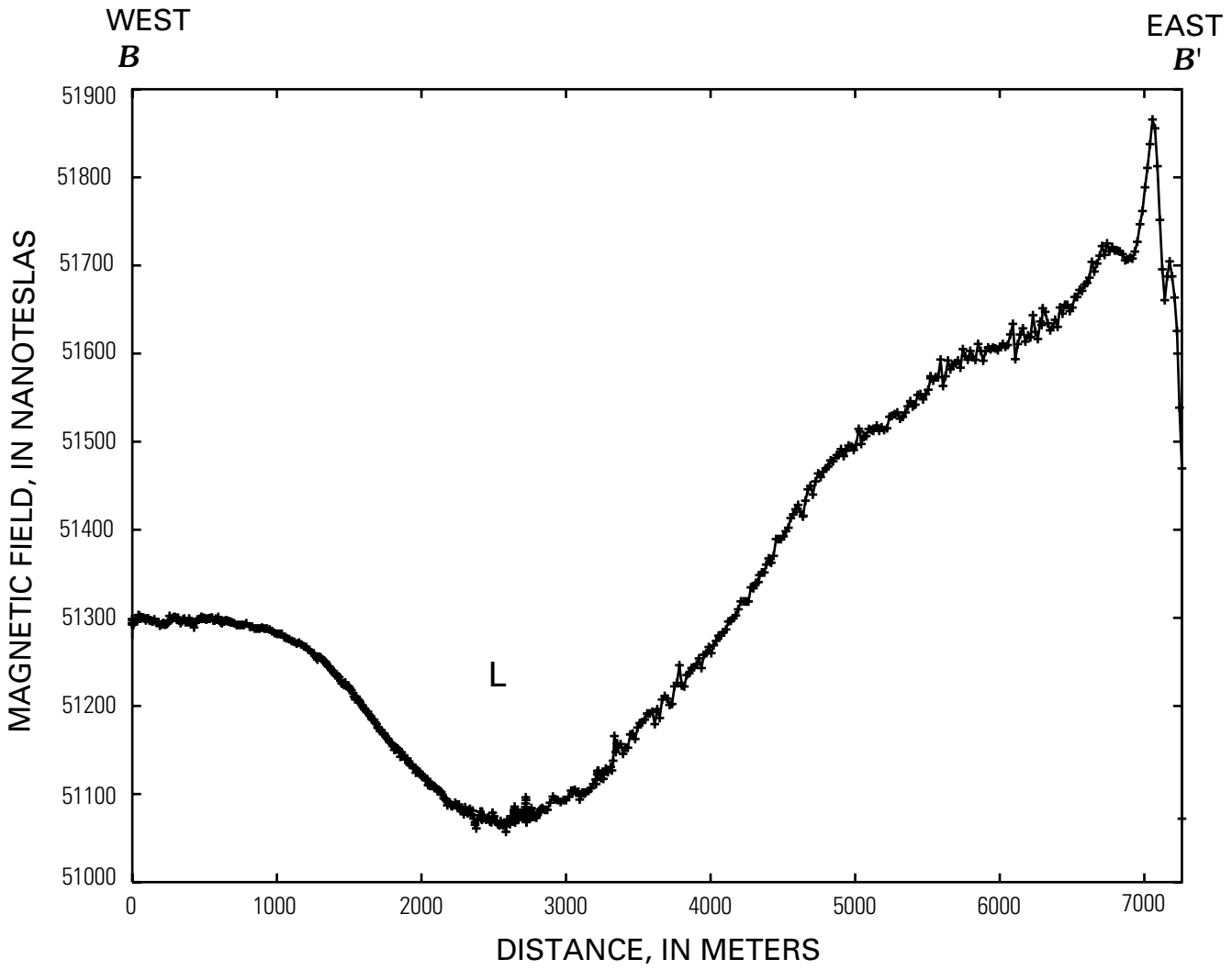

Figure 4. Ground magnetic profile *B*-*B*′ across magnetic low (marked L here and in fig. 3) east of Bare Mountain fault. Sensor 2.4 m above ground surface. East end of profile terminates at drill USW VH-1.

magnetic anomalies that depend on the thickness and magnetization of the individual tuff units (Bath and Jahren, 1984). North-south-trending anomalies are present over mapped normal faults at Yucca Mountain (Bath and Jahren, 1984). This pattern of anomalies also extends west of Yucca Mountain (and its mapped faults) halfway across southern Crater Flat, and to within a distance of 4–5 km east of the Bare Mountain range-front fault across northern Crater Flat (fig. 3). This relation suggests that faults offsetting the underlying tuff units extend at least halfway across Crater Flat. The difference in magnetic anomaly patterns between northern and southern Crater Flat, which is approximately on trend with an east-west-trending gravity gradient (just north of profile *A*-*A*′ in fig. 1), may indicate a change in structural style between northern and southern Crater Flat.

The southwest edge of Crater Flat is dominated by a magnetic low (marked L in fig. 3). Drill hole VH-2 penetrated 30 m of reversely polarized basalt at 360-m depth (Carr and Parrish, 1985). The age and magnetic polarity of this basalt are the same as for basalt exposed along the south edge of Crater Flat. The continuity of the Crater Flat magnetic low to the south over exposed 10.5 Ma basalt suggests that the Crater Flat low is caused by reversely magnetized basalt. A ground magnetic profile across the magnetic low indicates that the basalt is not offset vertically by more than 50 m (fig. 4). This profile suggests that the low-angle fault shown in figure 2*B* cannot be a shallow-dipping surface consisting of multiple normal faults, unless the faults are older than 10.5–11 Ma or have offsets smaller than 50 m.

Magnetic data indicate that the west edge of the buried basalt at Crater Flat coincides with the modeled location of the step in the Bare Mountain fault (fig. 2*A*), as well as with the east edge of the east-trending magnetic anomalies associated with the Wood Canyon Formation. The magnetic data and the gravity data indicate that Precambrian and Paleozoic rocks of Bare Mountain extend farther east than the mapped range-front fault. The magnetic data, however, suggest that monolithologic breccias or low-angle normal faults are not the reason for the location of the gravity gradient. Landslide breccias might not preserve the coherence of the east-west-trending magnetic anomalies into the Crater Flat fill. These anomalies would not be abruptly terminated (as the magnetic data suggest) if a low-angle fault were the reason for the presence of pre-Cenozoic rock east of the Bare Mountain fault. The magnetic data thus appear to support the step or caldera model presented in figure 2*A*.

One piece of geophysical evidence used to support the caldera model is the magnetic high (marked H in fig. 3) present over central Crater Flat. Carr (1984, 1990) concluded that the source of the anomaly is a thick accumulation of normally polarized rocks of what was then called the Bullfrog Member (now raised to formation rank as the Bullfrog Tuff; Sawyer and others, 1994) of the Crater Flat Tuff (now the Crater Flat Group; Sawyer and others, 1994). Carr (1984, 1990) argued that this thickening of the Bullfrog is evidence for a caldera in Crater Flat and that the observed uplift of the Bullfrog between drill holes USW VH-1 and USW VH-2 is evidence of a resurgent dome. The minimum thickness of the Bullfrog Tuff, as measured in the USW VH-1 drill hole, is nearly the same as the maximum thickness measured in drill holes and outcrops at Yucca Mountain. The top of the formation is about 573 m higher in drill hole USW VH-1 than in USW VH-2 (Carr, 1982; Carr and Parrish, 1985). Modeling of the anomaly, using an average magnetization of 2 A/m based on measurements by Rosenbaum and Snyder (1984), suggests that Carr's (1990) proposed doming and increase in thickness of the Bullfrog are not enough to account for the magnetic high present over Crater Flat (fig. 5). The gradients of the magnetic high indicate that, if the Bullfrog is the source, an abrupt change in magnetization or thickness must take place within that formation. Modeling of the anomaly indicates that the top of the source actually may be much deeper than the observed top of the Bullfrog, perhaps as deep as the base of the basin fill. The possible source of the magnetic high could be either a Cretaceous or a Tertiary intrusion.

Conclusions

Because of the nonuniqueness of the potential field method, it is impossible to determine which of the three distinct gravity models described herein is the most appropriate on the basis of gravity studies alone. Nonetheless, gravity data can provide alternative models that can be tested by other geophysical methods. Analysis of the magnetic field over Crater Flat supports the stepped normal-fault model rather than the low-angle normal-fault or high-density alluvium models,

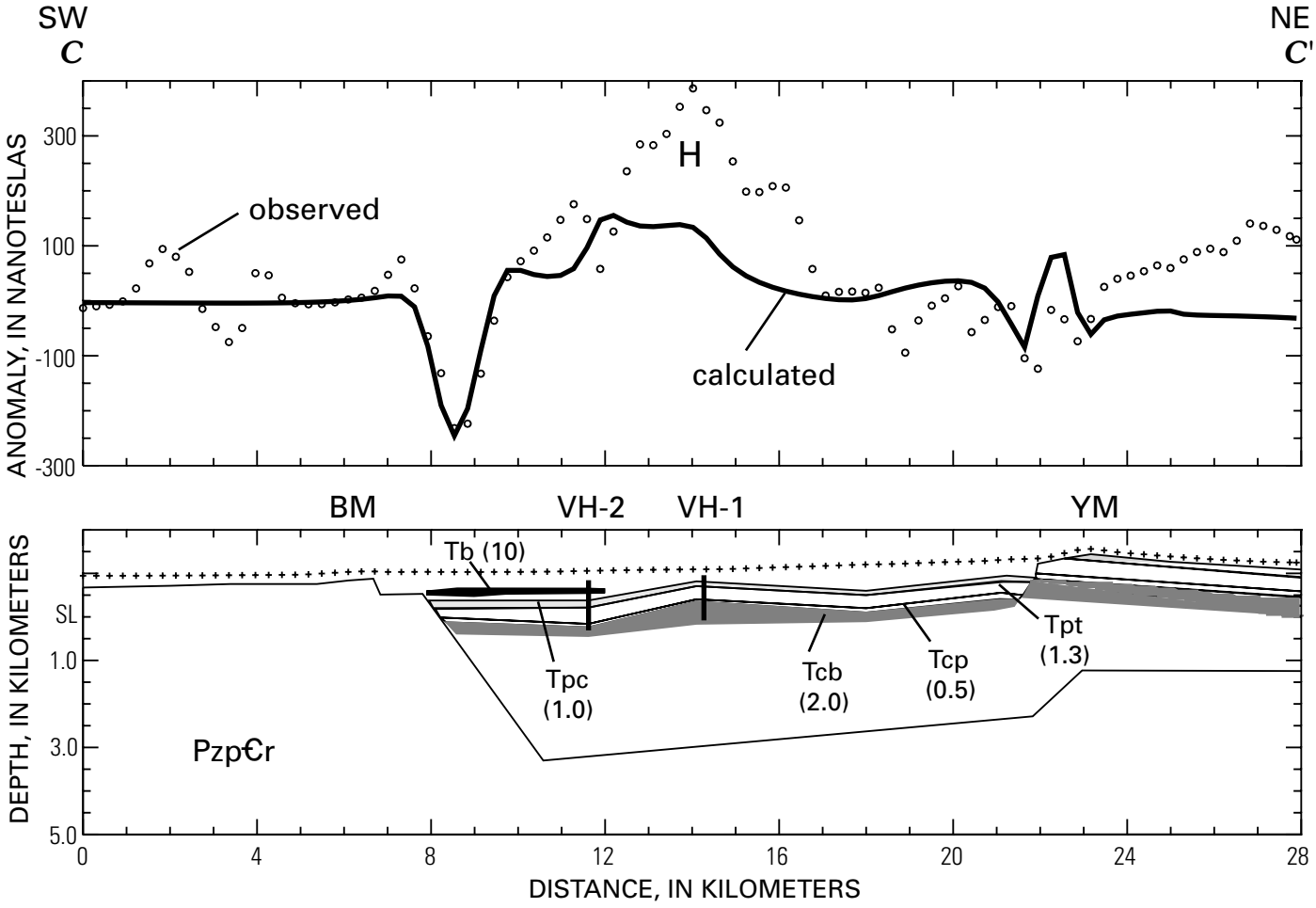

Figure 5. Simplified magnetic model across Crater Flat along profile *C-C'* (see fig. 3). Tb, Tertiary basalt; Tpc, Tiva Canyon Tuff of the Paintbrush Group; Tpt, Topopah Spring Tuff of the Paintbrush Group; Tcp, Prow Pass Tuff of the Crater Flat Group; Tcb, Bullfrog Tuff of the Crater Flat Group (shaded); PzpЄr, Precambrian and Paleozoic rocks. Numbers in parentheses are remanent magnetizations in amperes per meter from Rosenbaum and Snyder (1984). BM, Bare Mountain; YM, Yucca Mountain; H, magnetic high; VH-1 and VH-2, boreholes. Location of USW VH-2 projected onto profile. Gridded values are observed gravity data. Basement geometry inferred from gravity.

although the magnetic data do not eliminate these alternative models. Modeling of the Crater Flat magnetic high, previously cited as evidence for a resurgent dome within Crater Flat, suggests that the source of the anomaly may not be doming of the Bullfrog Tuff of the Crater Flat Group; the top of the source of the anomaly may be as deep as the floor of the basin fill and could be either a Cretaceous or a Tertiary intrusion.

References Cited

Ackermann, H.D., Mooney, W.D., Snyder, D.B., and Sutton, V.D., 1988, Preliminary interpretation of seismic-refraction and gravity studies west of Yucca Mountain, Nevada and California, *in* Carr, M.D., and Yount, J.C., eds., Geologic and hydrologic investigations of a potential nuclear waste disposal site at Yucca Mountain, southern Nevada: U.S. Geological Survey Bulletin 1790, p. 23–33.

Baldwin, M.J., and Jahren, C.E., 1982, Magnetic properties of drill core and surface samples from the Calico Hills area, Nye County, Nevada: U.S. Geological Survey Open-File Report 82-536, 27 p.

Bath, G.D., 1967, Aeromagnetic anomalies related to remanent magnetism in volcanic rocks, Nevada Test Site: U.S. Geological Survey Open-File Report 973, 20 p.

Bath, G.D., and Jahren, C.E., 1984, Interpretations of magnetic anomalies at a potential repository site located in the Yucca Mountain area, Nevada Test Site: U.S. Geological Survey Open-File Report 84-120, 40 p.

Blakely, R.J., and Simpson, R.W., 1986, Approximating edges of source bodies from magnetic or gravity anomalies: Geophysics, v. 51, p. 1494–1498.

Brocher, T.M., Carr, M.D., Fox, K.D., Jr., and Hart, P.E., 1993, Seismic reflection profiling across Tertiary extensional structures in the eastern Amargosa Desert, southern Nevada, Basin and Range province: Geological Society of America Bulletin, v. 105, p. 30–46.

Byers, F.M., Jr., Carr, W.J., Orkild, P.P., Quinlivan, W.D., and Sargent, K.A., 1976, Volcanic suites and related cauldrons of the Timber Mountain-Oasis Valley caldera complex, southern Nevada: U.S. Geological Survey Professional Paper 919, 70 p.

Carr, W.J., 1974, Summary of tectonic and structural evidence for stress orientation at the Nevada Test Site: U.S. Geological Survey Open-File Report 74-176, 53 p.

———1982, Volcano-tectonic history of Crater Flat, southwestern Nevada, as suggested by new evidence from drill hole USW VH-1 and vicinity: U.S. Geological Survey Open-File Report 82-457, 23 p.

———1984, Regional structural setting of Yucca Mountain, southwestern Nevada, and late Cenozoic rates of tectonic activity in part of the southwestern Great Basin, Nevada and California: U.S. Geological Survey Open-File Report 84-854, 109 p.

———1990, Styles of extension in the Nevada Test Site region, southern Walker Lane Belt—An integration of volcano-tectonic and detachment fault models, *in* Wernicke, B.P., ed., Basin and Range extensional tectonics near the latitude of Las Vegas, Nevada: Geological Society of America Memoir 176, p. 283–303.

Carr, W.J., Byers, F.M., Jr., and Orkild, P.P., 1984, Stratigraphic and volcano-tectonic relations of Crater Flat Tuff and some older volcanic units, Nye County, Nevada: U.S. Geological Survey Open-File Report 84-114, 42 p.

Carr, W.J., and Parrish, L.D., 1985, Geology of drill hole USW VH-2, and structure of Crater Flat, southwestern Nevada: U.S. Geological Survey Open-File Report 85-475, 41 p.

Carr, W.J., Waddell, S.J., Vick, G.S., Stock, J.M., Monsen, S.A., Harris, A.G., Cork, B.W., and Byers, F.M., Jr., 1986, Geology of drill hole UE25p#1—A test hole to pre-Tertiary rocks near Yucca Mountain, southern Nevada: U.S. Geological Survey Open-File Report 86-175, 87 p.

Cordell, Lindrith, 1985, Techniques, applications, and problems of analytical continuation of New Mexico aeromagnetic data between arbitrary surfaces of very high relief [abs.]: Proceedings of the International Meeting on Potential Fields in Rugged Topography, Institute of Geophysics, University of Lausanne, Switzerland, Bulletin no. 7, p. 96–99.

Grauch, V.J.S., Kucks, R.P., and Bracken, R.E., 1993, Aeromagnetic data for western areas of the Pahute Mesa and Beatty 30×60 minute quadrangles, Nye County, Nevada: EROS Data Center Magnetic Tape A0804, 3 p.

Hamilton, W.B., 1988, Detachment faulting in the Death Valley region, California and Nevada, *in* Carr, M.D., and Yount, J.C., eds., Geologic and hydrologic investigations of a potential nuclear waste disposal site at Yucca Mountain, southern Nevada: U.S. Geological Survey Bulletin 1790, p. 51–85.

Harris, R.N., Ponce, D.A., Healey, D.L., and Oliver, H.W., 1989, Principal facts for about 16,000 gravity stations in the Nevada Test Site and vicinity: U.S. Geological Survey Open-File Report 89-682A, 78 p.

Healey, D.L., Clutsom, F.G., and Glover, D.A., 1984, Borehole gravity meter surveys in drill holes USW G-3, UE-25p#1, and UE-25c#1, Yucca Mountain area, Nevada: U.S. Geological Survey Open-File Report 84-672, 16 p.

Kane, M.F., and Bracken, R.E., 1983, Aeromagnetic map of Yucca Mountain and surrounding regions, southwest Nevada: U.S. Geological Survey Open-File Report 83-616, 19 p., 1 pl., scale 1:48,000.

Labotka, T.C., and Albee, A.L., 1990, Uplift and exposure of the Panamint metamorphic complex, California, *in* Wernicke, B.P., ed., Basin and Range extensional tectonics near the latitude of Las Vegas, Nevada: Geological Society of America Memoir 176, p. 345–362.

Langenheim, V.E., Carle, S.F., Ponce, D.A., and Phillips, J.D., 1991, Revision of an aeromagnetic survey of the Lathrop Wells area, Nevada: U.S. Geological Survey Open-File Report 91-46, 17 p., 3 pl., scale 1:62,000.

Monsen, S.A., Carr, M.D., Reheis, Marith, and Orkild, P.P., 1992, Geologic map of Bare Mountain, Nye County, Nevada: U.S. Geological Survey Miscellaneous Investigations Map I-2201, scale 1:24,000, 6 p.

Mooney, W.D., and Schapper, Scott, 1995, Seismic refraction studies (Chapter 5), *in* Oliver, H.W., Ponce, D.A., and Hunter, W. C., eds., Major results of geophysical investigations at Yucca Mountain and vicinity, southern Nevada: U.S. Geological Survey Open-File Report 95-74, 274 p.

Nelson, P.H., Muller, D.C., Schimschal, Ulrich, and Kibler, J.E., 1991, Geophysical logs and core measurements from forty boreholes at Yucca Mountain, Nevada: U.S. Geological Survey Geophysical Investigations Map GP-1001, 10 sheets [accompanied by 64 p. text].

Okaya, D.A., and Thompson, G.A., 1985, Geometry of Cenozoic extensional faulting—Dixie Valley, Nevada: Tectonics, v. 4, no. 1, p. 107–125.

Oliver, H.W., and Fox, K.F., 1993, Structure of Crater Flat and Yucca Mountain, southeastern Nevada, as inferred from gravity data: American Nuclear Society Proceedings of the Fourth Annual International Conference on High Level Nuclear Waste Management, April 26-30, 1993, Las Vegas, Nevada, v. 2, p. 1812–1817.

Rosenbaum, J.G., and Snyder, D.B., 1984, Preliminary interpretation of paleomagnetic and magnetic property data from drill holes USW G-1, G-2, GU-3, G-3, and VH-1 and surface localities in the vicinity of Yucca Mountain, Nye County, Nevada: U.S. Geological Survey Open-File Report 85-49, 73 p.

Saltus, R.W., 1988, Gravity data for the state of Nevada on magnetic tape: U.S. Geological Survey Open-File Report 88-433, 20 p.

Saltus, R.W., and Blakely, R.J., 1993, HYPERMAG—An interactive 2- and 2 1/2-dimensional gravity and magnetic modeling program, version 3.5: U.S. Geological Survey Open-File Report 93-287, 39 p.

Sawyer, D. A., Fleck, R.J., Lanphere, M.A., Warren, R.G., Broxton, D.E., and Hudson, M. R., 1994, Episodic caldera volcanism in the Miocene southwestern Nevada volcanic field; Revised stratigraphic framework, $^{40}Ar/^{39}Ar$ geochronology, and implications for magmatism and extension: Geological Society of America Bulletin, v. 106, p. 1304–1318.

Scott, R.B., 1990, Tectonic setting of Yucca Mountain, southwest Nevada, *in* Wernicke, B.P., ed., Basin and Range extensional tectonics near the latitude of Las Vegas, Nevada: Geological Society of America Memoir 176, p. 251–282.

Simpson, R.W., Jachens, R.C., Blakely, R.J., and Saltus, R.W., 1986, A new isostatic residual gravity map of the conterminous United States with a discussion on the significance of isostatic residual anomalies: Journal of Geophysical Research, v. 91, p. 8348–8372.

Snyder, D.B., and Carr, W.J., 1984, Interpretation of gravity data in a complex volcano-tectonic setting, southwestern Nevada: Journal of Geophysical Research, v. 89, no. B12, p. 10193–10206.

Swadley, WC, and Carr, W.J., 1987, Geologic map of the Quaternary and Tertiary deposits of the Big Dune quadrangle, Nye County, Nevada, and Inyo County, California: U.S. Geological Survey Miscellaneous Investigations Map I-1767, scale 1:48,000.

Telford, W.M., Geldart, L.O., Sheriff, R.E., and Keyes, D.A., 1976, Applied geophysics: New York, Cambridge University Press, 960 p.

U.S. Geological Survey, 1979, Aeromagnetic survey of the Timber Mountain area, Nevada: U.S. Geological Survey Open-File Report 79-587, scale 1:62,500, three sheets.